Since January 2020 Elsevier has created a COVID-19 resource centre with free information in English and Mandarin on the novel coronavirus COVID-19. The COVID-19 resource centre is hosted on Elsevier Connect, the company's public news and information website.

Sensors and Actuators B 193 (2014) 334–339

Contents lists available at ScienceDirect

Sensors and Actuators B: Chemical

journal homepage: www.elsevier.com/locate/snb

General

Investigation of C-terminal domain of SARS nucleocapsid protein–Duplex DNA interaction using transistors and binding-site models

You-Ren Hsu[a], Yen-Wen Kang[a], Jung-Ying Fang[a], Geng-Yen Lee[b], Jen-Inn Chyi[b], Chung-ke Chang[c], Chih-Cheng Huang[a], Chen-Pin Hsu[a], Tai-huang Huang[c], Yu-Fen Huang[d], Yuh-Chang Sun[d], Chia-Hsien Hsu[e], Chih-Chen Chen[e], Sheng-Shian Li[a], J. Andrew Yeh[a], Da-Jeng Yao[a], Fan Ren[f], Yu-Lin Wang[a,*]

[a] Institute of Nanoengineering and Microsystems, National Tsing Hua University, Hsinchu, 300, Taiwan, ROC
[b] Department of Electrical engineering, National Central University, Jhongli, Taoyuan 32001, Taiwan, ROC
[c] Institute of Biomedical Sciences, Academia Sinica, Nankang, Taipei 11529, Taiwan, ROC
[d] Department of Biomedical Engineering and Environmental Science, National Tsing Hua University, Hsinchu 300, Taiwan, ROC
[e] Division of Medical Engineering, National Health Research Institutes, MiaoLi, Taiwan, ROC
[f] Department of Chemical Engineering, University of Florida, Gainesville, FL 32611, USA

ARTICLE INFO

Article history:
Received 20 November 2012
Received in revised form
12 November 2013
Accepted 17 November 2013
Available online 1 December 2013

Keywords:
SARS
GaN
HEMTs
Sensors
Dissociation constants
Binding sites

ABSTRACT

AlGaN/GaN high electron mobility transistors (HEMTs) were used to sense the binding between double stranded DNA (dsDNA) and the severe acute respiratory syndrome coronavirus (SARS-CoV) nucleocapsid protein (N protein). The sensing signals were the drain current change of the HEMTs induced by the protein–dsDNA binding. Binding-site models using surface coverage ratios were utilized to analyze the signals from the HEMT-based sensors to extract the dissociation constants and predict the number of binding sites. Two dissociation constants, K_{D1} = 0.0955 nM, K_{D2} = 51.23 nM, were obtained by fitting the experimental results into the two-binding-site model. The result shows that this technique is more competitive than isotope-labeling electrophoretic mobility shift assay (EMSA). We demonstrated that AlGaN/GaN HEMTs were highly potential in constructing a semiconductor-based-sensor binding assay to extract the dissociation constants of nucleotide–protein interaction.

The breakout of severe acute respiratory syndrome (SARS) in 2002 caused a large mortality and almost paralyzed the world economy in 2003. More than 8000 probable infected cases and 774 deaths were reported worldwide ranging 29 countries, according to World Health Organization (WHO) [1]. This disease is caused by the SARS coronavirus. A coronavirus protein, nucleocapsid protein (N protein), encapsidates the coronavirus genomic RNA playing an important role in the virus replication. SARS-N protein has been shown its capability of interacting with RNA and DNA, and therefore is known as a nucleic acid binding protein [2–5]. Investigating the nucleotide-SARS-N protein interaction can help us to explore the virus genome packaging process to construct a genome packaging model for SARS coronavirus. Electrophoretic mobility shift assay (EMSA) and filter binding assay have been widely used to study protein–nucleic acid interaction in the last 30 years [6–9]. However, these two methods require labeling of fluorescent probes or isotope elements on nucleic acids to provide signals for quantitative molecule detection. Thus, the cost for these methods is high, and the labeling may alter the binding affinity of molecules. Developing an efficient and molecule-labeling free binding assay with low cost and high sensitivity becomes a very important issue.

AlGaN/GaN high electron mobility transistors (HEMTs) have been successfully demonstrated for detection of gases, chemicals, and biomolecuels [10–17]. The AlGaN/GaN HEMT sensors have shown high sensitivity due to the high concentration of two-dimensional electron gas induced by the piezoelectric polarization of the strained AlGaN layer and the spontaneous polarization [10,15,17]. The gate region of the HEMTs can be modified or immobilized with various sensing materials to interact with analytes, which result in potential change on gate area leading to the current change of transistors. Gallium nitride (GaN) is thermally stable because of the wide-bandgap property. Devices made of GaN can

* Corresponding author. Tel.: +886 3 5162405.
E-mail address: ylwang@mx.nthu.edu.tw (Y.-L. Wang).

0925-4005/$ – see front matter © 2013 Elsevier B.V. All rights reserved.
http://dx.doi.org/10.1016/j.snb.2013.11.087

operate up to 500 °C. GaN is also chemically stable. Most acids and bases cannot etch GaN in regular condition. Only molten NaOH or KOH is known to be able to etch GaN. Therefore GaN-based sensors are particularly suitable for detection with salt, ions, chemicals, or biomolecules in liquid. The AlGaN/GaN HEMT-based sensors are excellent candidates for detection under harsh environments such as in buffered solution, serum, or in sea. In addition to the good thermal and chemical stability, the AlGaN/GaN HEMT has advantages such as real-time detection, fast response, high sensitivity, small size, light-weight, low cost and good reliability. These advantages ensure the AlGaN/GaN HEMT-based sensors to be an excellent platform to investigate the binding affinity of ligand–receptor complexes.

The AlGaN/GaN HEMTs are not only can be used as biosensors to detect various biomolecules, but can also be used to study the binding affinity of ligand–receptor complexes. The ligand–receptor pairs may include antigen-antibody, DNA–DNA, protein–DNA, protein–RNA, protein–protein, drug–protein, or substrate/inhibitor–enzyme systems. On the gate region of the HEMT sensors, receptors are usually immobilized to detect the ligand concentration in the bulk solution. The sensing mechanism is through the ligand–receptor affinity, which can be quantitatively expressed as equilibrium constant (affinity constants) or dissociation constants. Besides, a receptor may bind with more than one ligand, and each binding site on the receptor may have a unique dissociation constant with the ligand. With a quantitative analysis of the signals from the sensors through binding-site models, we are able to reveal how many binding sites are on the receptor (dsDNA) for certain ligands (SARS-N protein) and what the dissociation constants are for ligand–receptor complexes. Due to the fast response and low price of the AlGaN/GaN HEMT sensors, the analysis can be quickly done and the information about the ligand–receptor binding affinity can be obtained with very low expenses. Conventional methods to study ligand–receptor interactions also include enzyme-linked immunosorbent assay (ELISA) [18], isothermal titration calorimetry (ITC) [19,20], ultra-violet/visible light (UV/VIS) spectrum [21], surface plasmon resonance (SPR) [22,23], total internal reflection ellipsometry (TIRE) [24], and high-performance liquid chromatography (HPLC) [25]. Typically, ELISA and UV/VIS spectrum require labeling probes. ITC usually needs a large amount of sample. The commercial equipment (BIAcore) utilizing SPR technology has been used to characterize binding affinity of ligand–receptor complexes [17]. However, the equipment is expensive and therefore the cost for research is high. TIRE or HPLC also have good performances, but their prices are much higher than that of AlGaN/GaN HEMT sensors. In sharp contrast, the AlGaN/GaN HEMT sensors can achieve very good performances as the above mentioned while in the meantime keep a very low cost for research.

To investigate the number of binding sites and the dissociation constants of a receptor, the surface coverage ratio is adopted in one-binding-site model or multiple-binding-site model. The surface coverage ratio means the ratio of the number of ligand-bound receptors to the total number of receptors on the sensor. The ratio is related to the bulk concentration of the ligand, which is associated with the magnitude of the signals from the sensor. Dissociation constants are extracted by fitting experimental results into the binding-site models, and the number of binding sites on the receptors is obtained.

In this study, SARS-N protein–dsDNA binding pair is studied in the binding affinity with the theoretical binding-site models and the experimental results. One-binding-site mode and two-binding-site model are fitted with experimental results. The analysis of the signals from AlGaN/GaN HEMT sensors using the binding-site models demonstrates that the AlGaN/GaN HEMTs cannot only be used as biosensors, but also can be used to study the biological binding affinity of ligand–receptor pairs. Here AlGaN/GaN HEMTs were immobilized with dsDNA on gate region as the receptors for binding SARS-N proteins. The dsDNA is a 41-base dsDNA sequence from SARS coronavirus genome (base pairs 29,580 to 29,621) [5,26] which is conjugated to a 20-mer poly-dT single stranded DNA (ssDNA) tail to its 3′-end in one of the single strand of the dsDNA. The SARS-N protein can be divided into two binding domains, the C-terminal domain (CTD) and the N-terminal domain (NTD). Both the two domains can bind with nucleic acids through their electropositive region. In this study, the SARS-N protein that we used has the CTD only. The sensors were used to study the affinity between the CTD and the dsDNA.

Methods

Fabrication of AlGaN/GaN HEMTs

The HEMT structure consisted of a 3 μm-thick undoped GaN buffer, 150 Å-thick undoped $Al_{0.25}Ga_{0.75}N$ and 10 Å-thick undoped GaN cap layer. The AlGaN layer was designed to induce high spontaneous polarization, which generated a two-dimensional electron gas beneath the AlGaN layer. The epilayers were grown by metal–organic chemical vapor deposition (MOCVD) on sapphire substrates. Mesa isolation was performed using an inductively coupled plasma (ICP) etching system with Cl_2/BCl_3 gases under ICP power of 300 W at 2 MHz and a process pressure of 10 mTorr. Ohmic contacts ($60 \times 60\ \mu m^2$) separated with gaps of 30 μm consisted of e-beam deposited Ti/Al/Ni/Au and was annealed at 850 °C, 45 s under flowing N_2. 100 Å-thick gold was deposited on the gate region. Photoresist of 1.8 μm (Shipley S1818) was used to encapsulate the source/drain regions, with only the gate region open to allow the liquid solutions to cross the surface.

DNA surface immobilization

The ssDNA molecules 5′-thiol-TTTTTTTTTTTTTTTTTTTTTTCATCGAGGCCACGCGGAGTACGATCGAGGGTACAGTGAA-3′, and 3′AAGTAGCTCCGGTGCGCCTCATGCTAGCTCCCATGTCACTT-5′) were purchased from Genomics (Taipei, Taiwan). The dsDNA was hybridized by these two ssDNA molecules in TE Buffer (30 mM Tris–HCl, pH = 8.0, 30 mM NaCl, 1 mM EDTA, 25 mM TCEP (tris(2-carboxyethyl)phosphine). Then, the dsDNA solution was dropped on the gate area of AlGaN/GaN HEMTs, and waited for 30 h. The free dsDNA was washed away with phosphate buffer (10 mM sodium phosphate, pH = 6.0, 50 mM NaCl, 1 mM EDTA).

Sensor measurement

The characteristics of source–drain current–voltage of the sensor was measured at 25 °C using an Agilent B1500 parameter analyzer with the gate region exposed. The source-drain bias was fixed at 0.35 V. Different concentrations of the SARS N-protein CTD were sequentially dropped on the sensor in a real-time measurement.

Results and discussion

Fig. 1(a) and (b) shows the schematics and the plan-view of the SARS-N protein sensor, respectively. Fig. 2 shows the real-time measurement of the SARS-N protein at constant bias of 350 mV for the sensor. Phosphate buffered saline (10 mM sodium phosphate pH 6.0, 50 mM NaCl, 1 mM EDTA) was initially dropped on the sensor. There is no net current change until the target protein concentration of 0.003 nM of the protein was added. A clear current change was observed as the system reached a steady

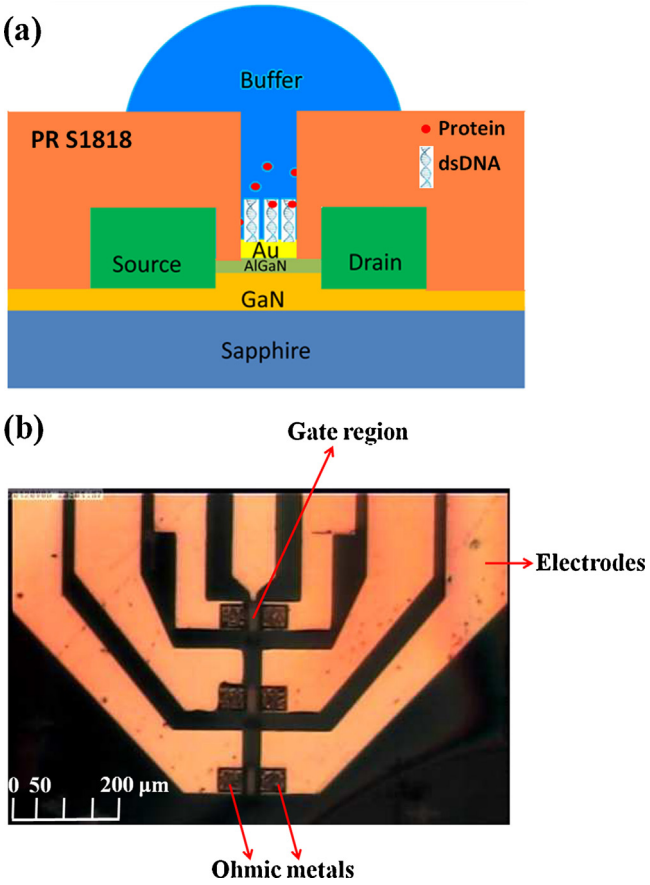

Fig. 1. (a) Schematics of the N protein sensor. (b) Plan-view photography of the sensor.

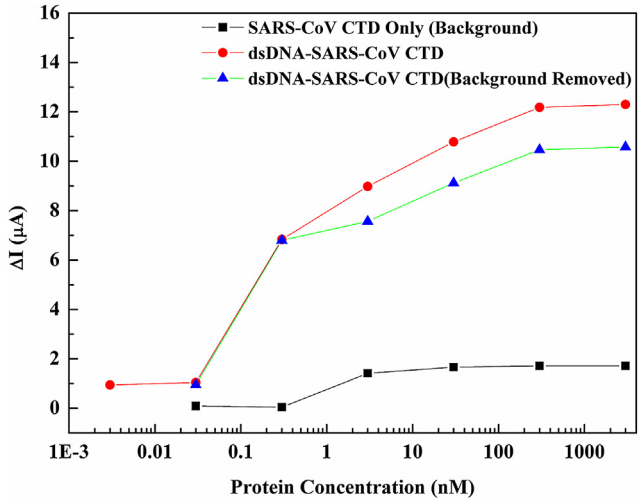

Fig. 3. Current changes at different concentrations of N protein CTD in log scale. The red line and the black line represent the current changes from the HEMT with and without DNA immobilized, respectively. The green line is the net current by subtracting the black line from the red line. (For interpretation of the references to colour in this figure legend, the reader is referred to the web version of this article.)

state. Real-time current monitoring spanned the range of protein concentrations from 0.003 nM to 3000 nM, and showed saturation as the concentration of N protein larger than 300 nM. The current drop for different protein concentration was due to the binding between the protein and the dsDNA on the gate region of the transistor, resulting in the change of the surface potential on the gate region, leading to the drain current drop. The protein concentration in Fig. 2 was an accumulated concentration. Therefore, the current drop for each target protein concentration was determined by the difference of the current levels between the steady state of the target concentration and the steady state of the buffer solution. The red lines in Fig. 2 represent the average current level for each steady state. Fig. 3 shows the current changes at different SARS-N protein-CTD concentrations from the sensors. The red line and the black line represent the current changes from the HEMT with and without DNA immobilized, respectively. The green one is the net current by subtracting the black line from the red line.

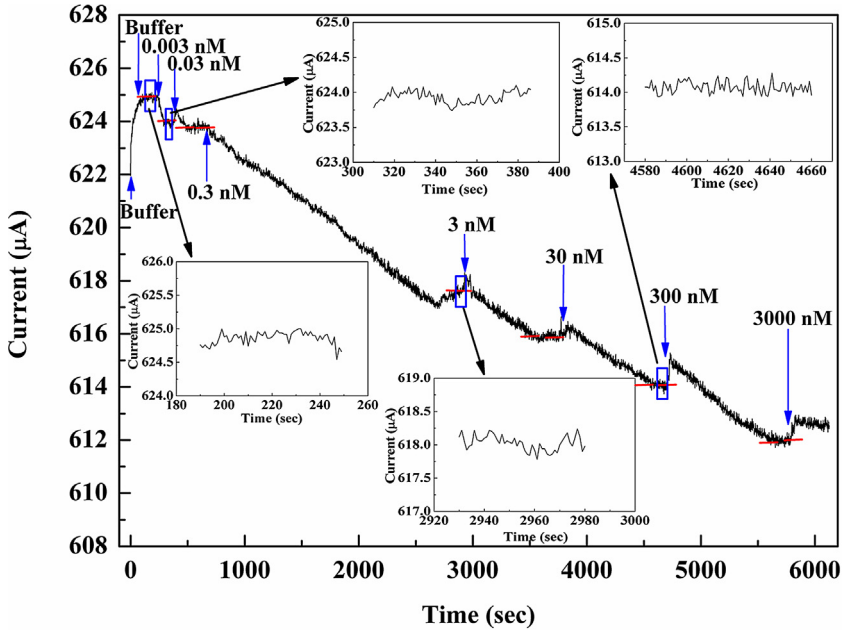

Fig. 2. Real-time detection of the N protein from 0.003 nM to 3000 nM at constant bias of 350 mV. (For interpretation of the references to colour in this figure legend, the reader is referred to the web version of this article.)

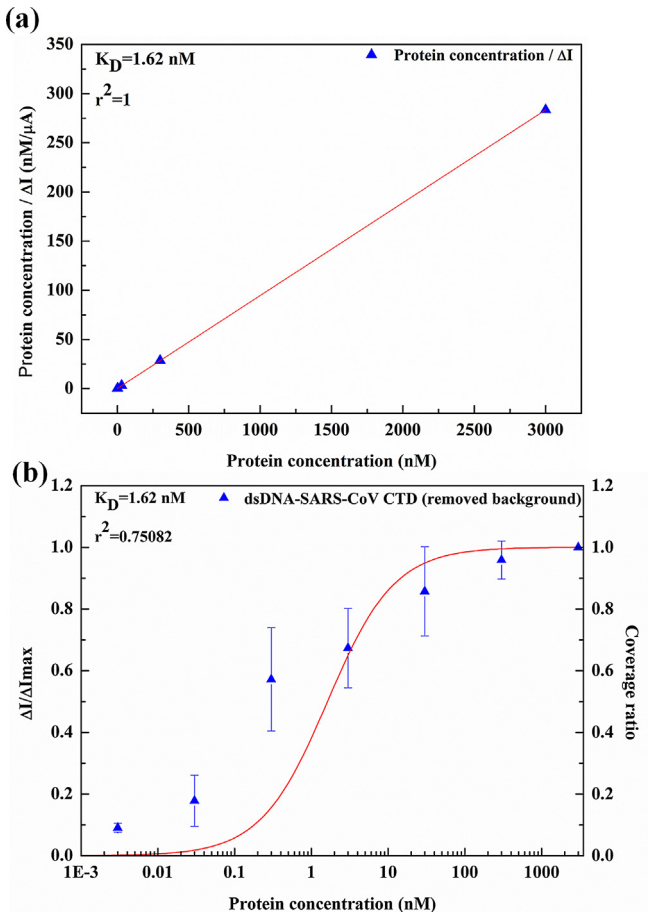

Fig. 4. (a) Dissociation constant extracted from the linear regression of Langmuir isotherm equation (b) Surface coverage ratio as a function of the protein concentration calculated with the dissociation constant extracted from (a). The $\Delta I/\Delta I_{max}$ from the experiment are shown as dots versus protein concentration.

The chemical reaction for the surface-immobilized receptor (dsDNA) and the free ligand (SARS-N protein-CTD) in bulk solution can be expressed as the following equations:

$$[R] + [L] \leftrightarrow [RL] \tag{1}$$

$$K = K_A = \frac{1}{K_D} = \frac{[RL]}{[R][L]} \tag{2}$$

where K is the equilibrium constant for formula (1), K_A is the association constant, and K_D is the dissociation constant. $[R]$ is the concentration of the unbound receptor immobilized on the sensor surface. $[L]$ is the ligand concentration in the bulk solution. $[RL]$ is the concentration of the ligand–receptor complex on the sensor surface.

To estimate the dissociation constant, the Langmuir isotherm equation was usually used to extract the dissociation constant by linear regression [27–30]. Here the current changes were introduced to the Langmuir equation for calculating the dissociation constant.

$$\frac{[L]}{\Delta I} = \frac{[L]}{\Delta I_{max}} + \frac{K_D}{\Delta I_{max}} \tag{3}$$

where ΔI is the current change at the bulk concentration of ligand $[L]$, and ΔI_{max} is the saturated current change. The dissociate constant can be extracted from the linear regression by using Eq. (3), as shown in Fig. 4(a). The extracted dissociation constant from the linear regression was obtained as 1.62×10^{-9} M.

The Langmuir equation shown in Eq. (3) can be rearranged as the following expression:

$$\frac{\Delta I}{\Delta I_{max}} = \frac{1}{1 + K_D/[L]} \tag{4}$$

The right-hand side of Eq. (4) is equal to the ratio of ligand–receptor complex concentration $[RL]$ to the total receptor concentration $[R]_{max}$. Here this ratio is defined as the surface coverage ratio α, as shown in Eq. (5).

$$\frac{1}{1 + K_D/[L]} = \frac{[RL]}{[R]_{max}} \equiv \alpha \tag{5}$$

Here the total receptor concentration is the sum of the unbound receptor concentration and the ligand–receptor complex concentration. The equation is shown as $[R]_{max} = [R] + [RL]$.

Fig. 4(b) shows the curve of surface coverage ratio from Eq. (5) using the dissociation constant extracted from Fig. 4(a) and the $\Delta I/\Delta I_{max}$ obtained from the experimental results shown as dots versus the ligand concentration in log scale. It is obvious that the curve of the surface coverage ratio does not match well with those experimental dots. From Eq. (5), it is shown that the surface coverage ratio actually depends on the ratio of dissociation constant to the concentration of ligand, that is $K_D/[L]$. When K_D equals 10 folds or 10% of $[L]$, the surface coverage ratio goes to around 9.09% and 90.91%, respectively. Beyond 90.91% or below 9.09% of the surface coverage ratio, increasing or decreasing the concentration of antigen does not change the surface coverage ratio much. Therefore, we conclude that for a one-binding-site model, the most significant change of the surface coverage ratio is within the range of the ligand concentration between one order higher and one order lower than the value of the dissociation constant. This was also shown by experimental data in literature [29]. Thus, ideally once the dissociation constant is determined, the highest sensitivity for the sensor is only within this two-order range of ligand concentration. On the other hand, for any experimental result, the surface coverage ratio between 9.09% and 90.91% should only cover two orders of ligand concentration for an ideal one-binding-site model. However, in Fig. 4(b), it is significant that between 9.09% and 90.91% of the surface coverage, the experimental data points cover more than 3 orders of the ligand concentration. Therefore, it is not possible to fit these experimental points well into the surface coverage ratio with the one-binding-site model. The wide range of the ligand concentration within that coverage ratio (9.09–90.91%) may be resulted from multiple binding sites of the receptor. Compared with Fig. 4(a), Fig. 4(b) is clearly more sensitive to see whether the one-binding-site model can really fit into the experimental data. Thus, the surface coverage ratio versus the ligand concentration will be used for finding out the number of binding sites and the associated dissociation constants. Here a two-binding-site model is proposed as the following.

In the two-binding-site model, the chemical equations are described as below, (6)$[R]_{site1} + [L] \leftrightarrow [RL]_{site1}$ K_{D1}

$$[R]_{site2} + [L] \leftrightarrow [RL]_{site2} \quad K_{D2} \tag{7}$$

where the K_{D1} and K_{D2} are the dissociation constants for the two binding sites on a receptor. The total current change is assumed to be the sum of the current change resulted from ligand–receptor complex at site 1 and at site 2, respectively, as shown in Eqs. (8) and (9).

$$\Delta I = \Delta I_1 + \Delta I_2 \tag{8}$$

$$\Delta I = \frac{\Delta I_{max\,1}[L]}{K_{D1} + [L]} + \frac{\Delta I_{max\,2}[L]}{K_{D2} + [L]} = \frac{\Delta I_{max\,1}}{K_{D1}/[L] + 1} + \frac{\Delta I_{max\,2}}{K_{D2}/[L] + 1} \tag{9}$$

$$\Delta I = \alpha_1 \Delta I_{max\,1} + \alpha_2 \Delta I_{max\,2} \tag{10}$$

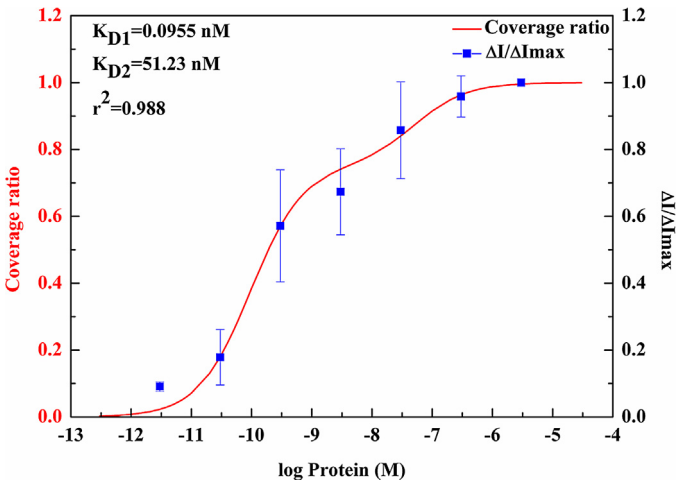

Fig. 5. The curve-fitting of the two-binding-site model with surface coverage ratio at different SARS-N protein-CTD concentrations and the two dissociation constants extracted from the model.

where α_1 and α_2 are the surface coverage ratio at site 1 and site 2 of the receptor.

Let the left and the right side of Eq. (10) be divided by ΔI_{max}, and define $\alpha \equiv \Delta I/\Delta I_{max}$, $c_1 \equiv \Delta I_{max\,1}/\Delta I_{max}$, and $c_2 \equiv \Delta I_{max\,2}/\Delta I_{max}$. The α in this two binding-site model represents the overall surface coverage ratio. It is obvious that c_1 and c_2 are constants, and $c_1 + c_2 = 1$. Then we can get Eq. (11), as follows:

$$\alpha = \alpha_1 c_1 + \alpha_2 c_2 \tag{11}$$

Fig. 5 shows the surface coverage ratio at different N protein concentrations from the average of three measurements and the curve-fitting for a two-binding-site model. The experimental data points nicely fit into the two-binding-site model. Two dissociation constants, (K_{D1} = 0.0955 nM, K_{D2} = 51.23 nM, c_1 = 0.7506, and c_2 = 0.2494) were extracted from the two-binding-site model. The correlation coefficient r^2 is 0.988. This result suggests that there are at least two SARS-N protein-CTD binding on the dsDNA. It was not reported the dissociation constants between the dsDNA and the SARS-N protein-CTD. However, it was observed in literature [5] that both RNA and dsDNA have very strong binding with the SARS-N protein-CTD, while the ssDNA has weaker binding compared with RNA and the dsDNA. RNA aptamer was reported to have a dissociation constant as 0.8 nM when binding to the SARS-N protein-CTD [31]. There is only single dissociation constant obtained due to the extraction of the dissociation constant simply from a one-binding-site system. The value of the dissociation constant for RNA from the literature [31] is just between our K_{D1} and K_{D2}. Since both dsDNA and RNA have strong binding affinity with the SARS-N protein-CTD, we believe that the values of our dissociation constants are in a reasonable range. In another literature, ssDNA aptamer was reported to have dissociation constant as 4.9 nM when binding to the SARS-N protein-CTD [32]. Although the sequence of the RNA aptamer and the ssDNA aptamer is different from ours, the values of the reported dissociation constants are consistent with our results. Our results are obtained based on dealing with the whole system with full spectrum of the protein concentration.

Chemically, the formula for this reaction may usually be expressed as Eqs. (12) and (13).

$$[R] + [L] \leftrightarrow [RL] \quad K_{D1} \tag{12}$$

$$[RL] + [L] \leftrightarrow [RL_2] \quad K_{D2} \tag{13}$$

It may be argued that whether three-binding-site model or even higher number of binding-sites should be considered. To investigate that possibility, three-binding-site model was used to fit the experimental data, and it looks like the fitting is also very nice, as shown in Appendices A and B. However, we can easily find that for the three dissociation constants extracted from the three-binding-site model, the K_{D2} and the K_{D3} are very close, and their values are almost the same as the K_{D2} extracted from the two-binding-site model. Needless to say, the K_{D1} extracted from the three-binding-site model is almost the same as the K_{D1} extracted from the two-binding-site model. We therefore can conclude that if two-binding-site model can be well fitted with the experimental data, it is not necessary to try with higher number of binding-site model. The methodology that we adopt in the analysis of the dissociation constants and the number of binding sites in this research mainly relies on the full range of the protein concentration, from low surface coverage to full saturation, which allows us to see the whole response for full range of the protein concentration. This is a very important key to investigate the complete information about the affinity between the protein and the dsDNA. If the sensor was only tested with a small range of the protein concentration, but not the full range until saturation, then the information about the number of binding sites and the dissociation constants extracted from the curve-fitting technique may be misled into wrong results and conclusion. We found that for some researches the range of the ligand concentration is sometimes ignored. To investigate the full range of the ligand concentration, the model that utilizes the surface coverage ratio is very successful to handle such many orders of magnitude of the ligand concentration. Therefore, the binding-site model using the surface coverage ratio together with the HEMTs becomes a simple and useful tool for the analysis of the binding affinity between the SARS-N-protein and dsDNA.

In conclusions, AlGaN/GaN HEMTs immobilized with dsDNA have been used to bind SARS-N protein-CTD, and to elucidate the number of binding sites on the dsDNA and the dissociation constants. Two dissociation constants, K_{D1} = 0.0955 nM, K_{D2} = 51.23 nM, were obtained by fitting the experimental results into the two-binding-site model. The AlGaN/GaN HEMTs and the binding-site models were demonstrated to be very efficient and cheap tools to investigate the information of the number of binding sites on dsDNA for the SARS N-protein CTD and the dissociation constants which is important for studying the SARS virus genome packaging process.

Acknowledgment

This work was partially supported by National Science Council grant (No. 99B20495A) and by the research grant (100N2049E1) at National Tsing Hua University. We thank Dr. Jen-Inn Chyi, and Dr. Chung-ke Chang and Dr. Tai-huang Huang for providing us the AlGaN/GaN epi wafers and the SARS-N protein, respectively, and for consulting as well.

Appendix A. Supplementary data

Supplementary data associated with this article can be found, in the online version, at http://dx.doi.org/10.1016/j.snb.2013.11.087.

References

[1] K. Stadler, V. Masignani, M. Eickmann, S. Becker, S. Abrignani, H.-D. Klenk, et al., SARS-beginning to understand a new virus, Nature Reviews Microbiology 1 (2003) 209–218.
[2] K.S. Saikatendu, J.S. Joseph, V. Subramanian, B.W. Neuman, M.J. Buchmeier, R.C. Stevens, et al., Ribonucleocapsid formation of severe acute respiratory syndrome coronavirus through molecular action of the N-terminal domain of N protein, Journal of Virology 81 (2007) 3913–3921.
[3] C.-k. Chang, Y.l. Hsu, Y.h. Chang, F.a. Chao, M.C. Wu, Y.s. Huang, et al., Multiple nucleic acid binding sites and intrinsic disorder of SARS coronavirus

nucleocapsid protein-implication for ribonucleocapsid protein packaging, Journal of Virology (2008), JVI.02001-08.
[4] M. Takeda, C.-k. Chang, T. Ikeya, P. Güntert, Chang Y.-h., Y.-l. Hsu, et al., Solution structure of the C-terminal dimerization domain of SARS coronavirus nucleocapsid protein solved by the SAIL-NMR method, Journal of Molecular Biology 380 (2008) 608–622.
[5] C.-Y. Chen, C.-k. Chang, Y.-W. Chang, S.-C. Sue, H.-I. Bai, L. Riang, et al., Structure of the SARS coronavirus nucleocapsid protein RNA-binding dimerization domain suggests a mechanism for helical packaging of viral RNA, Journal of Molecular Biology 368 (2007) 1075–1086.
[6] L.S. Klig, I.P. Crawford, C. Yanofsky, Analysis of trp repressor–operator interaction by filter binding, Nucleic Acids Research 15 (1987) 5339–5351.
[7] M.M. Garner, A. Revzin, A gel electrophoresis method for quantifying the binding of proteins to specific DNA regions: application to components of the *Escherichia coli* lactose operon regulatory system, Nucleic Acids Research 9 (1981) 3047–3060.
[8] M. Fried, D.M. Crothers, Equilibria and kinetics of lac repressor–operator interactions by polyacrylamide gel electrophoresis, Nucleic Acids Research 9 (1981) 6505–6525.
[9] M.G. Fried, M.A. Daugherty, Electrophoretic analysis of multiple protein–DNA interactions, Electrophoresis 19 (1998) 1247–1253.
[10] P. Gangwani, S. Pandey, S. Haldar, M. Gupta, R.S. Gupta, Polarization dependent analysis of AlGaN/GaN HEMT for high power applications, Solid-State Electronics 51 (2007) 130–135.
[11] M. Eickhoff, J. Schalwig, G. Steinhoff, O. Weidemann, L. Görgens, R. Neuberger, et al., Electronics and sensors based on pyroelectric AlGaN/GaN heterostructures—Part B: Sensor applications, Physica Status Solidi (c) Current Topics in Solid State Physics 0 (2003) 1908–1918.
[12] M. Eickhoff, R. Neuberger, G. Steinhoff, O. Ambacher, G. Müller, M. Stutzmann, Wetting behaviour of GaN surfaces with Ga- or N-face polarity, Physica Status Solidi (b) Basic Solid State Physics 228 (2001) 519–522.
[13] J. Schalwig, G. Müller, O. Ambacher, M. Stutzmann, Group-III-nitride based gas sensing devices, Physica Status Solidi (a) Applications and Material Science 185 (2001) 39–45.
[14] R. Neuberger, G. Müller, O. Ambacher, M. Stutzmann, High-electron-mobility AlGaN/GaN transistors (HEMTs) for fluid monitoring applications, Physica Status Solidi (a) Applications and Material Science 185 (2001) 85–89.
[15] R. Neuberger, G. Müller, O. Ambacher, M. Stutzmann, Ion-induced modulation of channel currents in AlGaN/GaN high-electron-mobility transistors, Physica Status Solidi (a) Applications and Material Science 183 (2001) R2–R10.
[16] S.J. Pearton, B.S. Kang, K. Suku, F. Ren, B.P. Gila, C.R. Abernathy, et al., GaN-based diodes and transistors for chemical, gas, biological and pressure sensing, Journal of Physics: Condensed Matter 16 (2004) R961.
[17] C. Bertucci, S. Cimitan, Rapid screening of small ligand affinity to human serum albumin by an optical biosensor, Journal of Pharmaceutical and Biomedical Analysis 32 (2003) 707–714.
[18] F. Orosz, J. Ovádi, A simple method for the determination of dissociation constants by displacement ELISA, Journal of Immunological Methods 270 (2002) 155–162.
[19] K. Chiad, S.H. Stelzig, R. Gropeanu, T. Weil, M. Klapper, K. Mullen, Isothermal titration calorimetry: a powerful technique to quantify interactions in polymer hybrid systems, Macromolecules 42 (2009) 7545–7552.
[20] M.A. Dobreva, R.A. Frazier, I. Mueller-Harvey, L.A. Clifton, A. Gea, R.J. Green, Binding of pentagalloyl glucose to two globular proteins occurs via multiple surface sites, Biomacromolecules 12 (2011) 710–715.
[21] Md Toro, R. Gargallo, R. Eritja, J. Jaumot, Study of the interaction between the G-quadruplex-forming thrombin-binding aptamer and the porphyrin 5,10,15,20-tetrakis-(*N*-methyl-4-pyridyl)-21,23*H*-porphyrin tetratosylate, Analytical Biochemistry 379 (2008) 8–15.
[22] J. Homola, Surface plasmon resonance sensors for detection of chemical and biological species, Chemical Reviews 108 (2008) 462–493.
[23] L. Choulier, Y. Nomine, G. Zeder-Lutz, S. Charbonnier, B. Didier, M.-L. Jung, D. Altschuh, Chemical library screening using a SPR-based inhibition in solution assay: simulations and experimental validation, Analytical Chemistry 85 (2013) 8787–8795.
[24] I. Baleviciute, Z. Balevicius, A. Makaraviciute, A. Ramanaviciene, A. Ramanavicius, Study of antibody/antigen binding kinetics by total internal reflection ellipsometry, Biosensors and Bioelectronics 39 (2013) 170–176.
[25] E. Pfaunmiller, A.C. Moser, D.S. Hage, Biointeraction analysis of immobilized antibodies and related agents by high-performance immunoaffinity chromatography, Methods 56 (2012) 130–135.
[26] M.A. Marra, S.J.M. Jones, C.R. Astell, R.A. Holt, A. Brooks-Wilson, Y.S.N Butterfield, et al., The genome sequence of the SARS-associated coronavirus, Science 300 (2003) 1399–1404.
[27] W.U. Wang, C. Chen, K-h. Lin, Y. Fang, C.M. Lieber, Label-free detection of small-molecule-protein interactions by using nanowire nanosensors, Proceedings of the National Academy of Sciences of the United States of America 102 (2005) 3208–3212.
[28] T.-W. Lin, P.-J. Hsieh, C.-L. Lin, Y.-Y. Fang, J.-X. Yang, C.-C. Tsai, et al., Label-free detection of protein-protein interactions using a calmodulin-modified nanowire transistor, Proceedings of the National Academy of Sciences of the United States of America (2009).
[29] K. Maehashi, K. Matsumoto, Y. Takamura, E. Tamiya, Aptamer-based label-free immunosensors using carbon nanotube field-effect transistors, Electroanalysis 21 (2009) 1285–1290.
[30] Y. Chen, H. Vedala, G.P. Kotchey, A. Audfray, S. Cecioni, A. Imberty, et al., Electronic detection of lectins using carbohydrate-functionalized nanostructures: graphene versus carbon nanotubes, ACS Nano 6 (2011) 760–770.
[31] D.-G. Ahn, I.-J. Jeon, J.D. Kim, M.-S. Song, S.-R. Han, S.-W. Lee, H. Jung, J.-W. Oh, RNA aptamer-based sensitive detection of SARS coronavirus nucleocapsid protein, Analyst 134 (2009) 1896–1901.
[32] S.-J. Cho, H.-M. Woo, K.-S. Kim, J.-W. Oh, Y.-J. Jeong, Novel system for detecting SARS coronavirus nucleocapsid protein using an ssDNA aptamer, Journal of Bioscience and Bioengineering 112 (2011) 535–540.

Biographies

You-Ren Hsu is a Ph.D. student in Institute of NanoEngineering and MicroSystems, National Tsing Hua University. His current research interests include semiconductor sensor based labeling free binding assay, and relative biophysical application using semiconductor devices.

Geng-Yen Lee is a Ph.D. student in Institute of Electrical Engineering, National Central University.

Jen-Inn Chyi received the B.S. and M.S. degrees in electrical engineering from National Tsing-Hua University, and the Ph.D. degree in electrical engineering from the University of Illinois, Urbana-Champaign. He serves as a Distinguished Lecturer of IEEE EDS since 2004. He is an Associate Editor of IEEE Photonics Technology Letters as well as an Overseas Editor of Japanese Journal of Applied Physics. Dr. Chyi is a member of Phi Tau Phi, and Fellow of IEEE and SPIE.

Chung-ke Chang received the Ph.D. degree in Carnegie Mellon University. Now Dr. Chang is a postdoctoral fellow in Institute of Biomedical Sciences, Academia Sinica,Taiwan. His field of research is Biophysical and biochemical properties of the SARS-CoV nucleocapsid protein, and TDP43 protein.

Chih-Cheng Huang was a master student in Institute of NanoEngineering and MicroSystems, National Tsing Hua University.

Chen-Pin Hsu is a Ph.D. student Institute of NanoEngineering and MicroSystems, National Tsing Hua University.

Tai-huang Huang is distinguished research fellow in Institute of Biomedical Sciences, Academia Sinica,Taiwan.

Yu-Fen Huang is an associate professor in Department of Biomedical Engineering and Environmental Science, National Tsing Hua University. Prof. Huang is interested in Capillary electrophoresis, Biosensors, Cell Imaging, and Targeted Drug delivery and Cancer therapy.

Yuh-Chang Sun is a professor in Department of Biomedical Engineering and Environmental Science, National Tsing Hua University.

Chia-Hsien Hsu is a research assistant in Division of Medical Engineering, National Health Research Institutes, MiaoLi, Taiwan, R.O.C.

Chih-Chen Chen is an assistant professor in Institute of NanoEngineering and MicroSystems, National Tsing Hua University.

Sheng-Shian Li is an associate professor in Institute of NanoEngineering and MicroSystems, National Tsing Hua University.

J. Andrew Yeh is a professor in Institute of NanoEngineering and MicroSystems, National Tsing Hua University.

Da-Jeng Yao is a professor in Institute of NanoEngineering and MicroSystems, National Tsing Hua University.

Fan Ren is Charles A. Stokes professor of Chemical Engineering at the University of Florida, Gainesville, FL, USA. Prior to joining UF in 1998, he worked for AT&T Bell Laboratories for 13 years as a Member of Technical Staff. His current research interests include semiconductor based sensors, Sb based HBTs and nitride Based HEMTs .He is a Fellow of ECS, APS and AVS.

Yu-Lin Wang is an assistant professor in Institute of NanoEngineering and MicroSystems, at National Tsing Hua University. He received his Ph.D. degree in materials science and engineering at University of Florida in 2009. His current research interests include advanced wide bandgap electronics, photonics, and biosensors.